

Rapid characterisation of suspensions for waste treatment and resource recovery

Authors

J Wardrop¹, S J Baldock¹, I Coote², R Demaine², P R Fielden¹ and A D Martin^{3*}

*Corresponding author

¹Chemistry, Lancaster University, Lancaster, LA1 4YB, UK

²Crown Paints Limited, Crown House, Hollins Road, Darwen, Lancashire, BB3 0BG

³Engineering, Lancaster University, Lancaster, LA1 4YW, UK

Abstract

A simple device for the conduct of stepped pressure filtration measurements is described together with methods for making the empirical measurements and interpreting the data obtained. The data interpretation method applies a multi-step systematic approach, with each step supported by statistical justification, to characterise: filter cake particle stress, filtration diffusivity and cake hydraulic resistivity from a single stepped pressure experiment. The methods enable different flocculant materials to be more rapidly and more appropriately screened than conventional jar tests and large scale filtration trials. The methods are applied to the characterisation of a paint residue treated with aluminium sulphate and “PolyClay”.

The work shows that the addition of “PolyClay” as a filter aide reduces the hydraulic resistivity at lower solids concentrations but increases it at higher concentrations whilst simultaneously increasing the particle stress. Together these have a combined deleterious effect on the time and energy required to dewater the residues to high solids concentration by filtration. The results also show that a significant change in suspension behaviour occurs between the “PolyClay” doses of 140 mg l⁻¹ and 660 mg l⁻¹ and that further changes up to “PolyClay” doses of 1600 mg l⁻¹ are more modest. The results indicate the existence an opportunity to reduce “PolyClay” dose into a range between 10% and 50% of current practice. In addition the results provide evidence that alternative, centrifuge based, technology is worthy of investigation.

Background

Particulate suspensions are a common by-product or process intermediate in many industrial processes. It can often be advantageous to separate these suspensions into their constituent raw materials to increase the economic viability of a process. Multiple processes exist to enable this such as filtration, evaporation, centrifugation. Worldwide the coatings industries make extensive use of “engineered” suspensions whose properties make any wastes or residues arising difficult to treat or successfully recycle. Water borne paints have helped to reduce the environmental impact associated with solvents but achieved little with regard to the solid polymers, pigments and adjuncts. The costs of disposal of treated wastes are typically levied in accordance with the wet mass. “Aggressive” treatment processes designed to maximise the elimination of water typically have the coincident effect of rendering both the solids and the water more difficult to recycle. Crown Paints is a major UK based decorative paints manufacturer. As is typical for large fast moving consumer goods, “FMCG”, manufacturing processes are generally batch or short run continuous. Such operations

typically give rise to high volumes of waste from cleaning and product change over activities. Continuous, commodity, minerals processing operations also give rise to substantial quantities of waste materials in the form of suspensions. These residuals by their nature and quantity must be safely disposed of in the environment. This activity necessitates understanding the characteristics of the suspensions in order to cost effectively dewater and subsequently safely store the resultant cake. A key waste stream arising from Crown Paints' manufacture of water based paints is process washings. The company currently dewater this material via a conventional coagulation using aluminium sulphate followed by flocculation with a modified bentonite clay, "PolyClay" [CTech Europe 2020], and finally a pressure filtration process.

Buscall & White [1987] developed the idea of compressive yield stress $Py(\varphi)$ to characterise the resistance of a flocculated suspension to further compression. It defines the minimum pressure required to obtain a filter cake of specific volumetric concentration, φ . $Py(\varphi)$ was expected to be dependent on the arrangement of inter-particle interactions. In this work the volumetric concentration, φ , is substituted for the mass concentration analogue, c . A sample suspension of concentration, φ or c is contained within a device comprising a cylinder closed at top with a piston and at the bottom with a porous membrane to yield an initial suspension height, h_0 . A differential, filtration pressure, ΔP is applied to the piston driving the filtration process, forcing the liquid through the filtration membrane. After a sufficient time period the system reaches an equilibrium condition where the pressure from the piston is fully supported by the structure of the filter cake. Replicating this process over multiple pressures is used to characterise the $Py(c)$ curve. The hydraulic resistivity, $r(c)$, whose reciprocal is commonly termed the "permeability" is characterised by the product of the hydrodynamic drag on an isolated particle, r_0 , and the so-called hindered settling function. this parameter characterises hydrodynamic resistance to flow through the suspension network structure as a function of solids concentration. Established methods to determine $Py(c)$ and $r(c)$ experimentally are variously described by De Kretser et al [2001], Kynch [1952] and Landman & White [1994].

As performing multiple experiments to determine $Py(c)$ and $r(c)$ is arduous and time consuming a stepped filtration method to reduce characterisation time was proposed by De Kretser et al [2001] And validated by Usher et al [2001]. A typical stepped pressure filtration method requires two runs to fully characterise a sample (one to determine $Py(c)$ of the sample at a range of pressures & the other the permeability/hydraulic resistivity, $r(c)$). The method described here, takes the next logical step to simplify the method into a single filtration test.

A filtration device was built based on the designs in Green et al [1998] and De Kretser et al [2001]. Modifications to those designs include the accurate delivery of a specific pressure gravitationally rather than via a pneumatic cylinder.

Filtration apparatus

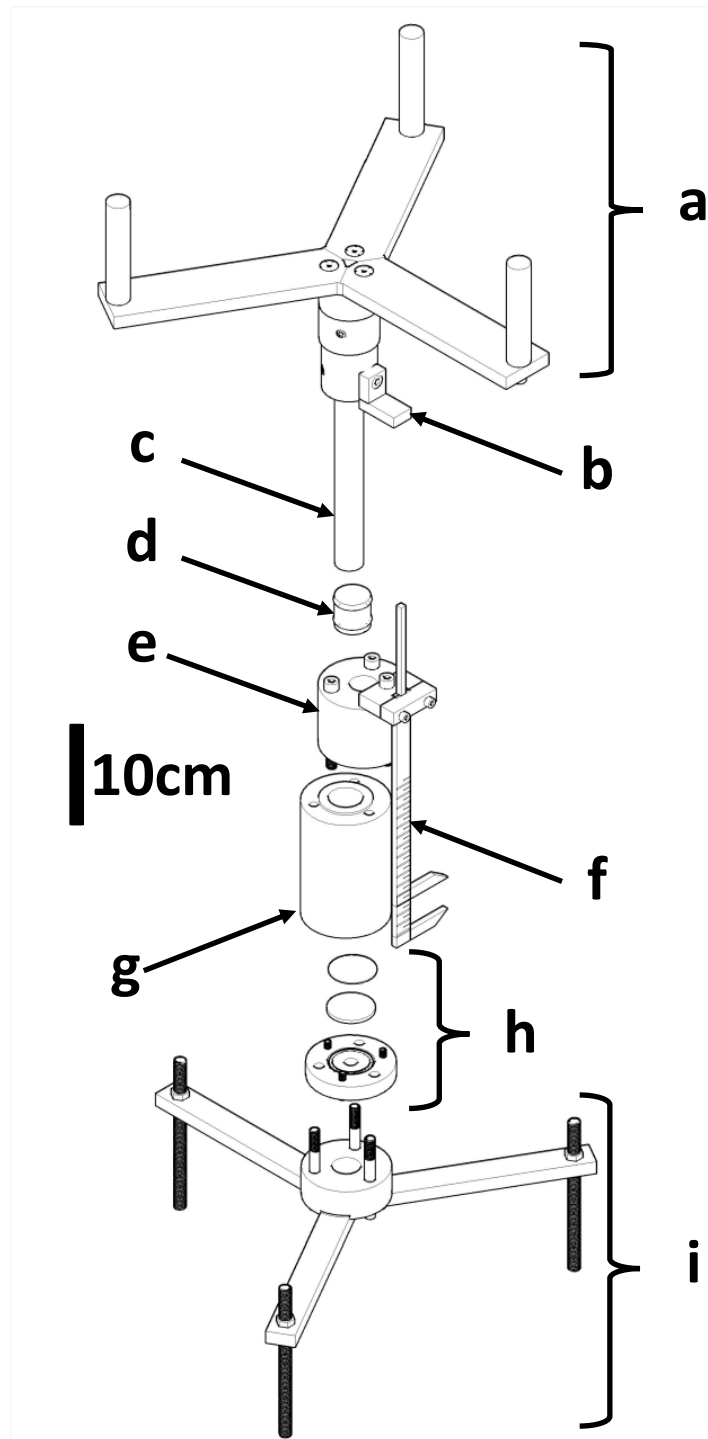


Figure 1 Schematic diagram of bench filter press. a, barrel assembly; b, digital calliper stop; c, plunger; d, piston; e, plunger guide; f, digital calliper; g, piston cylinder; h, filter assembly; i, support tripod assembly.

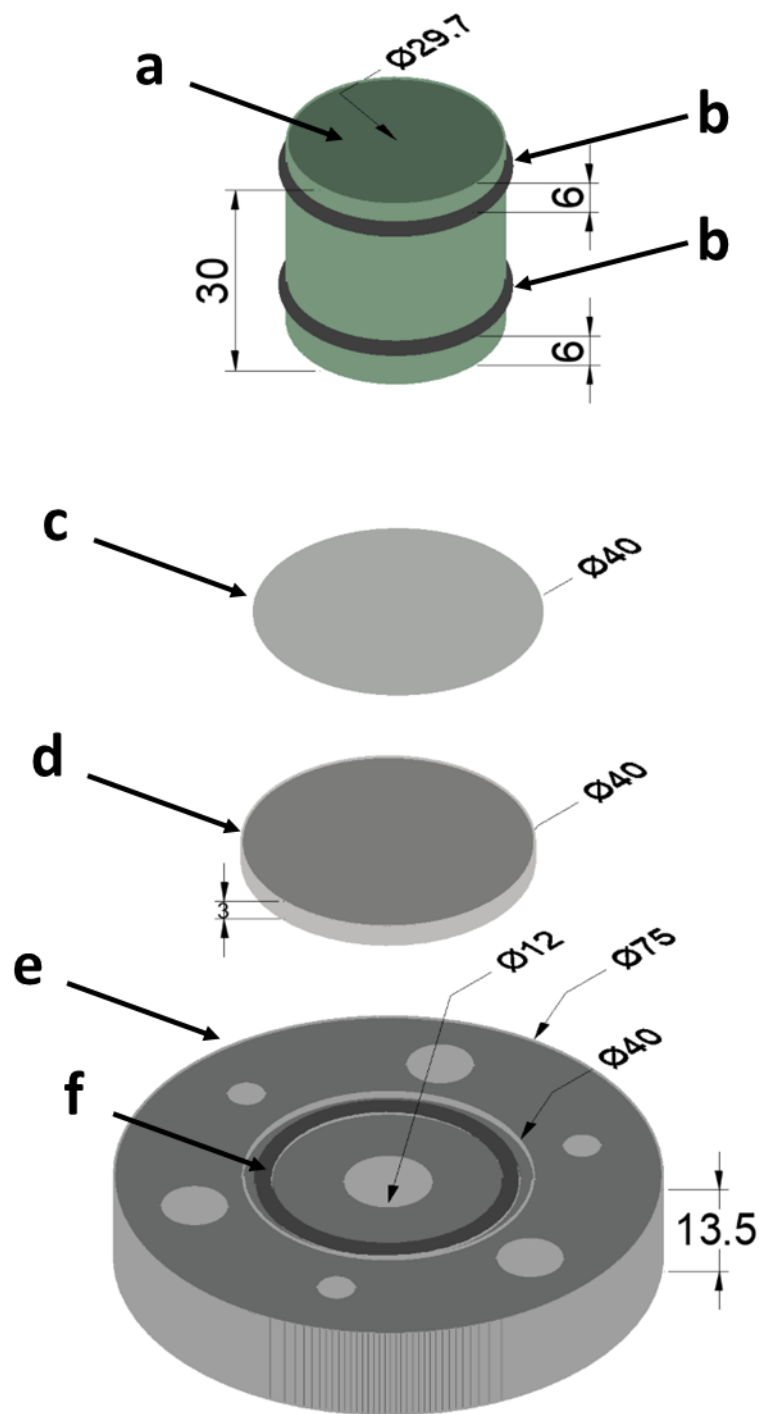


Figure 2 Detailed schematic of the filter assembly (dimensions in mm). a, is the Delrin® piston; b, is a Nitrile 70 O-ring; c, is a circle of filter press membrane fabric; d, is a porous sintered stainless steel support; e, is the piston cylinder end-cap; f, is a Nitrile 70 O-ring.

Figure 1 shows a schematic of the lab-scale filter press apparatus. The device is gravity driven to provide controlled and programmed pressure to the flocculated wastewater. The barrel assembly supports a 40 l plastic barrel (load reservoir) which receives programmed doses of water from a charge vessel in 1 l aliquots to add weights with a resolution of 0.997 kg. The assembly is fabricated from aluminium arms and nylon upright guides to hold the barrel in a fixed and centralised position. The linear movement of the barrel assembly, as the sample is forced through the filter assembly (h), is measured against the digital calliper stop (b). A plunger, fabricated from a brass bar (c) drives the Delrin® piston (d) through the piston cylinder (g). A perfect seal is provided by a pair of O-rings. The plunger guide (e) is fabricated from 303 stainless steel to ensure perpendicular drive between the plunger and piston. The linear progression of the piston is monitored using a USB-linked digital calliper (Moore and Wright “Digitronic” digital vernier calliper, with USB connectivity. With an accuracy of 0.02 mm and precision of 0.01 mm). The piston cylinder (g) is fabricated from 303 stainless steel, and is precision bored to 30 mm. The filter assembly (h) is shown in a detailed schematic in Figure 2. The apparatus is supported by an adjustable tripod arrangement (i), which is adjusted to ensure the bore of the piston cylinder is vertical.

Figure 2 shows the detailed design and dimensions of the filter assembly and piston. The filter press membrane used throughout this study is a Polypropylene Filtercloth (PP-365-OM, Lathams International). The sintered stainless steel support disc (Powder Filter Disc) was a sample supplied by Porvair Filtration Group Ltd. (Fareham, Hampshire, UK). The endcap is fabricated from 303 stainless steel. The O-rings (2 mm x 33 mm bore; nitrile 70 rubber) were procured from Simply Bearings Ltd., (Leigh, Lancashire, UK) The arrangement of the endcap is mirrored in the base of the piston cylinder, which includes an identical recess and sealing O-ring.

In operation, the piston cylinder was separated from both the support tripod assembly and components “a” to “e” (see figure 1). The piston was placed into the top end of the piston cylinder and the whole unit inverted. The sample was then loaded and the piston manually pushed until the sample liquor was at the level of the O-ring seal in the base of the piston cylinder. The filter assembly was then carefully introduced and the endcap added and secured with three M6 303 stainless steel hex-bolts. The bolts were tightened until the O-rings were fully compressed within their recesses, which was designed to coincide with the tight clamping of the endcap onto the base of the piston cylinder. The piston unit was then inverted into its correct orientation, slipped onto the three support prongs of the support tripod assembly. The plunger, with the barrel assembly was carefully added such that the only force applied to the piston was the weight of the components of the assembly above the piston cylinder. Finally, the 40 l plastic water barrel was placed securely within the barrel assembly.

The digital calliper was linked with a laptop and was designed to transmit the length information directly into an Excel spreadsheet. The transmission would usually be triggered by a manual footswitch, which in our experiments was replaced by a CMOS analogue switch (CD4066) which itself was triggered by a switchable quartz crystal oscillator and frequency divider that gave a choice of 2; 1; 0.5; or 0.1 Hz. The experiment was initiated with the simultaneous activation of the trigger oscillator, such that the spreadsheet generated included the timeframe data in the vertical cell number, with the length data in each timeframe cell.

The weight added to the piston, via the plunger and weight of water held in the 40 l plastic barrel, was added by a programmable charge vessel that delivered exactly 1 l of water at a time determined by a simple time loop program executed from an Arduino UNO microcontroller. The microcontroller was pre-programmed according to the experiment design of the programmed plunger weight sequence.

Methods

Sample preparation

Mixtures, representative of paint residues, comprising 4% by volume paint were created using 20 ml (approx. 26.8 g) of Crown Retail Matt Emulsion Paint in 500 ml of DI water. The mixtures were agitated continuously to prevent sedimentation. A SI Analytics TitroLine 7750 & a 700 ml beaker was used to simulate a batch treatment tank. The pH of the residue mixtures were adjusted from approx. 8.4 to 6.3 using 3 g l⁻¹ aluminium sulphate (Sigma-Aldrich) to model the treatment process (typically requiring approx. 3-5 ml of aluminium sulphate solution). “PolyClay” flocculant was then dosed to each agitated mixture to achieve concentrations of 140 mg l⁻¹, 660 mg l⁻¹ and 1600 mg l⁻¹. These doses represented approximately 10%, 50% and 125% of the “PolyClay” dose typically used to treat residues from paint manufacture.

The treated suspension was slowly agitated for 300 seconds. After which a core sample (approx. 80ml) was extracted using a syringe.

Stepped pressure filtration

The filter cylinder and piston assembly was inverted and overfilled with approximately 80 ml of treated suspension to prevent the inclusion of air pockets before final closure by fitting of the filter membrane and support sinter. The closed filter assembly was then positioned into the tripod.

The stepped pressure filtration process was then initiated, following the pre-programmed sequence indicated in figure 3.

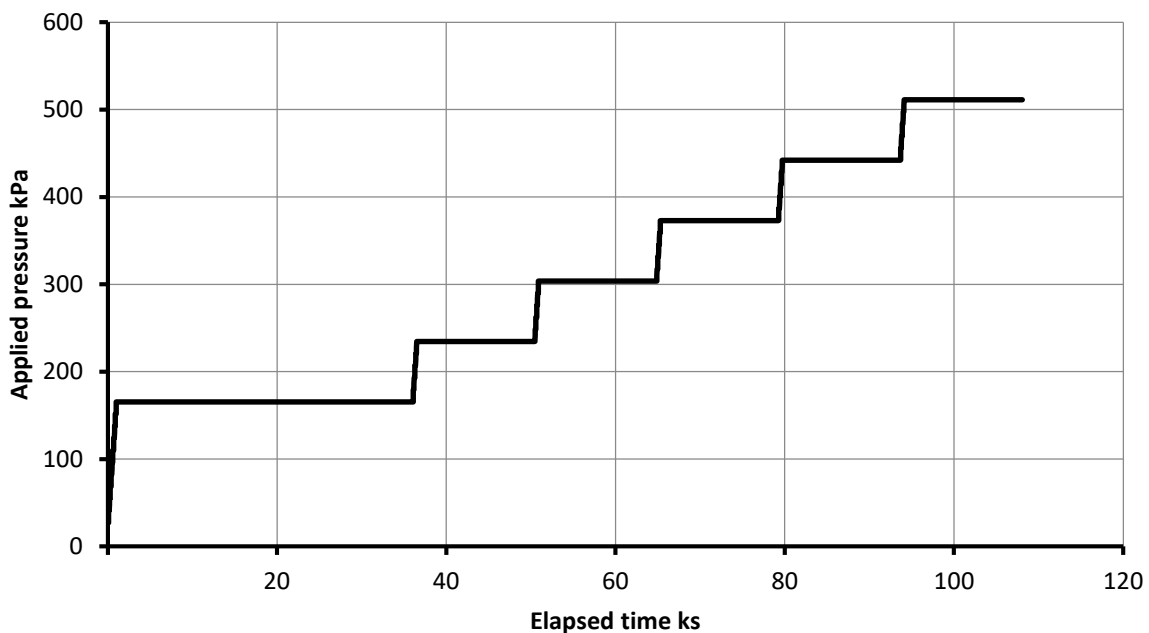


Figure 3 Stepped pressure programme

At the start of each pressure step the pressure was increased in a sequence of 5 sub-steps. Each sub-step comprised 2 phases: charge and ramp. The charge phase, lasting 80 seconds, comprised the filling of the calibrated charge vessel with a fixed mass (0.997 kg) of water, whilst the ramp phase, lasting 20 seconds, comprised draining the charge vessel into the load reservoir mounted on the piston assembly. During the ramp phase the fluid transfer was assumed to proceed at a constant rate leading to an assumed linear ramp of the applied pressure. Whilst this assumption is not correct it is of no consequence to the data collection. Throughout the “run” the piston height above datum was recorded every 0.5 s to yield height vs time data sets of the type shown in figure 4

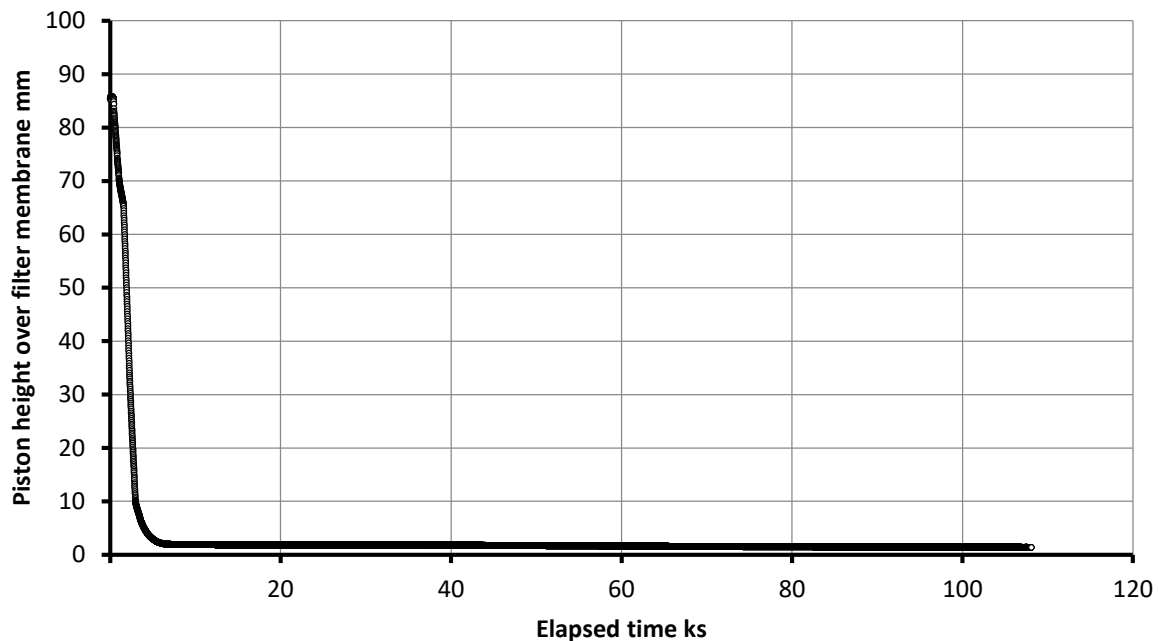


Figure 4 Typical height as a function of time data for a stepped pressure filtration “run”

Interpretation of the data

The height vs time data for each period of constant pressure was interpreted using a three step process.

Step 1: Cleaning of the data

Step 2: Interpretation of height versus time data for each applied pressure

Step 3: Interpretation of height versus time parameters as functions of concentration

Step 1

In the first step, the raw height versus time data was cleaned to remove “rogue” data pairs arising from electrical interference and to remove data when the pressure was unsteady or deviated from the set value. The clean data set was then subsampled at a frequency of 1:20 simply to improve the manageability.

Rogue data was identified by considering “frames” of subsamples of the raw data comprising 11 data pairs. The mean and standard deviation of these subsamples was calculated and the central data pair subjected to a significance test at the 0.95 level. A central data pair failing this test was flagged for subsequent removal before the sampling “frame” was advanced by 1 data pair.

Step 2

In the second step, the cleaned data was regressed to a sequence of increasingly detailed models the equations of which are set out in table 1. Each increase in complexity is characterised by the addition of one or more parameters. Progress through the sequence of models was determined by the “incremental F test” with a rejection criterion of 0.95.

N	Fitting parameters	Material properties accessible	Model
1	h_{∞}	c_{∞} , $Py(c_{\infty})$	$\hat{h} = h_{\infty}$
3	h_{∞}, M_L , t_{offset}	c_{∞} , $Py(c_{\infty})$, $D(c_{\infty})$, $r(c_{\infty})$	$\hat{h} = \hat{h}_L = h_{\infty} + (h^* - h_{\infty}) \sum_{n=1}^5 B_{L,n} e^{-(n-1/2)^2 M_L (t_R - t_C)}$ <p>Where</p> $B_{L,n} = \frac{4}{\pi^{3/2} (n - 1/2) \operatorname{erf}(\alpha)} \int_0^{\alpha} e^{-z^2} \cos\left\{(n - 1/2) \frac{\pi z}{\alpha}\right\} dz$ $h^* = \frac{h_{\infty} + \sqrt{\pi} \alpha e^{\alpha^2} \operatorname{erf}(\alpha) h_0}{1 + \sqrt{\pi} \alpha e^{\alpha^2} \operatorname{erf}(\alpha)}$ $t_C = \frac{\pi^2}{4 M_L \alpha^2} + t_{offset}$ <p>α is constrained to a fixed value of 2.69702</p>
4	h_{∞}, M_L , t_{offset}, α	c_{∞} , $Py(c_{\infty})$, $D(c_{\infty})$, $r(c_{\infty})$, $r(c^*)$	$\hat{h} = \begin{cases} t < t_C & \hat{h}_E = h_0 + C_E - \sqrt{C_E^2 + M_E (t_R - t_{offset})} \\ t \geq t_C & \hat{h}_L = h_{\infty} + (h^* - h_{\infty}) \sum_{n=1}^5 B_{L,n} e^{-(n-1/2)^2 M_L (t_R - t_C)} \end{cases}$ <p>Where $B_{L,n}, h^*$ and t_C are defined as for the 3 parameter model plus</p> $C_E = -(h_0 - h_C) \frac{((h_0 - h_C) + 2 M_L t_C \sum_{n=1}^5 (n - 1/2)^2 B_{L,n})}{2 ((h_0 - h_C) + M_L t_C \sum_{n=1}^5 (n - 1/2)^2 B_{L,n})}$ $M_E = \frac{(h_0 - h_C + C_E)^2 - C_E^2}{t_C}$ $h_C = (h^* - h_{\infty}) \sum_{n=1}^5 B_{L,n}$ <p>α is variable subject to the following constraint: $0 < \alpha < 2.69702$</p>

5	$h_{\infty}, M_L, t_{off}, \alpha, M_E$	$c_{\infty}, Py(c_{\infty}), D(c_{\infty}), r(c_{\infty}), r(c^*)$	$\hat{h} = \begin{cases} t < t_c & \hat{h}_E = h_0 + C_E - \sqrt{C_E^2 + M_E(t_R - t_{offset})} \\ t \geq t_c & \hat{h}_L = h_{\infty} + (h^* - h_{\infty}) \sum_{n=1}^5 B_{L,n} e^{-(n-1/2)^2 M_L(t_R - t_c)} \end{cases}$ <p>Where $B_{L,n}, h^*, h_c$ and α are defined as for the 4 parameter model plus</p> $t_c = \frac{(h_0 - h_c + C_E)^2 - C_E^2}{M_E}$ <p>M_E is variable subject to the following constraint: $0 < M_E$ C_E is constrained to a fixed value of zero</p>
---	---	--	---

Table 1. Filter piston height versus time models

The simple 1 parameter model permits the concentration dependent particle stress, $Py(c_{\infty})$, to be estimated even when there has been little or no filtration under the applied stage pressure. The 3 parameter model permits the interpretation of the data in terms of late or compression phase behaviour. The complimentary 3 parameter model interpreting the data in terms of early or Darcian phase behaviour was not found necessary in this work. The late phase model facilitated the estimation of the filtration diffusivity at the asymptotic concentration, $D(c_{\infty})$, in addition to the particle stress. Interpretation of $Py(c_{\infty})$ estimates as a function of concentration permitted subsequent estimation of the cake resistivity, $r(c_{\infty})$ under the same asymptotic conditions. The 4 and 5 parameter models permit the estimation of the cake resistivity at the diffusivity weighted mean cake concentration at cake completion, $r(c^*)$. The key difference between the two models lies in the consideration of the moment of cake completion, t_c . Both models consider the piston height, h , to be a continuous function of time. However, the 4 parameter model also considers the function to be “smooth” through the transition, i.e. the first derivative is also continuous. The 5 parameter model relaxes this constraint which, where statistically justified permits the model to describe the data more precisely with a concomitant development of a distinctive “kink” at cake completion and narrower confidence intervals for the estimated parameters. A potential final model introducing a 6th parameter by relaxing the constraint on C_E was not considered.

The models were implemented in Excel™ workbooks supported by additional VBA coding to systematically configure and run “SOLVER”. The squared unexplained residual, E_U^2 , was characterised by a linear sum of the un-weighted scalar differences between the estimated height, \hat{h} and the measured value, h squared.

$$E_U^2 = \sum (h - \hat{h})^2 \quad - 1$$

SOLVER was configured to minimise E_U^2 subject to the parameters and constraints of the specific model under consideration. Initially the unexplained residual around the 1 parameter model was established which is also known as the total variation and here temporarily denoted $E_U^2_{N-1}$. Then commencing with the 3 parameter model a test fit was made to establish the unexplained residual for this model, $E_U^2_N$ and the improvement was statistically tested using an incremental F statistic, F_{stat} , where:

$$F_{stat} = \frac{DoF_N}{E_U^2_N} \left\{ \frac{E_U^2_{N-1} - E_U^2_N}{DoF_{N-1} - DoF_N} \right\} \quad - 2$$

The calculated value of F_{stat} was then compared with the critical F statistic at the 0.95 level, F_{crit} , and the more complex model accepted when $F_{stat} > F_{crit}$. This procedure was then repeated for 4 and 5 parameter models. When $F_{stat} \leq F_{crit}$ the simpler model was accepted and the fitting procedure terminated.

Once the preferred model had been established and the “best fit” estimates of the parameters made the confidence limits of the estimates were made using the method of Kemmer and Keller [2010].

The confidence intervals for the derived material properties were then estimated using standard methods for the propagation of uncertainty.

This procedure was repeated for each set pressure to yield concentration dependent values for the material properties: $Py(c_\infty)$, $D(c_\infty)$ and $r(c^*)$.

Step 3

The three material properties estimated during the course of step 2 are not fully independent as the diffusivity, $D(c_\infty)$, is a function of the gradient of the particle stress and the cake resistivity. However at the asymptotic concentration it is the diffusivity that can be independently measured. Rather than the cake resistivity. In addition it is the particle stress, $Py(c)$ and the resistivity, $r(c)$, that are conventionally correlated with particle concentration. The interpretation proceeds according to 3 sub steps

Step 3a: Interpretation of the $Py(c)$ data as a function of solids concentration

Step 3b: Interpretation of the $r(c)$ data as a function of solids concentration

Step 3c: Correlation of filtration diffusivity, $D(c)$

Step 3a Interpretation of $Py(c)$ data

Three candidate models are defined in table 2 with 1, 2 and 3 parameters respectively, loosely based on thermodynamic concepts in which the particle stress is analogous to osmotic pressure

N	Coefficients	Form
1	\mathcal{R}^*	$Py = \mathcal{R}^* T c$
2	$\mathcal{R}^* \mathcal{D}^*, n_v$	$Py = \mathcal{R}^* T \mathcal{D}^* c^{n_v}$
3	$\mathcal{R}^*, \tilde{c}_{gel}, n_v$	<p>Where</p> $Py = \mathcal{R}^* T (c + \mathcal{B}^* c^2 + \mathcal{D}^* c^{n_v})$ $\mathcal{B}^* = -\frac{(n_v - 1)}{(n_v - 2)\tilde{c}_{gel}}$ $\mathcal{D}^* = \frac{1}{(n_v - 2)\tilde{c}_{gel}^{n_v - 1}}$

Table 2 Models of particle stress

The 1 parameter model is analogous to an ideal osmotic pressure relationship and the ideal gas law however with the concentration or reciprocal molar volume being expressed in terms of mass per unit volume the universal gas constant must be replaced by an analogous “specific gas constant”, \mathcal{R}^* . The 2 parameter model permits some description of non-ideal behaviour analogous to an equation of state of the form $Pv^n = \mathcal{R}T$. Finally the 3 parameter model is analogous to a simple virial equation of state. The number of parameters being minimised by arbitrarily constraining the particle

stress to pass through a minimum at $c = \tilde{c}_{gel}$ where the gel stress, $Py = \tilde{P}_{gel} = 0$. The choice of this functional form is quite arbitrary however it represents a simple continuous function which admits the possibility of a gel concentration and the coexistence of a dense particulate phase or floc and a rarefied suspension, a configuration routinely observed when conducting “jar testing” of coagulants and flocculants. However in this work observations of the particle stress at concentrations less than \tilde{c}_{gel} are not anticipated, thus the shape of the function in this region is not expected to carry any quantitative significance.

A method analogous to that used in the height versus time data is applied to the selection and fitting of the models to the data. The confidence band for the correlation and limits for the estimated parameters were calculated using the method of Kemmer and Keller [2010].

Step 3b Interpretation of the $r(c)$ data

A “measurement” of cake resistivity data, $r(c)$, can be derived from 2 sources: From the early stage filtration using the following expression:

$$r(c^*) = \left\{ \frac{(\Delta P - \Pi)(c^* - c_0)}{M_E c_0} \right\} \quad - 3$$

Where c^* is calculated from h^* using the following expression: $c^* = c_0 h_0 / h^*$, and from late stage filtration where,

$$\frac{r(c_\infty)}{\rho_s} = \frac{Py'(c_\infty)}{M_L} \frac{\pi^2}{h_\infty^2} \quad - 4$$

The data was interpreted using a modified Richardson-Zaki functional form:

$$r(c) = r_0 \left\{ 1 - \frac{c}{\rho_s} \right\}^{-n_{RZ}} \quad - 5$$

Where r_0 , ρ_s and n_{RZ} are candidate fitting parameters. Under the circumstances of the work reported here it is not possible, a priori, to assign a value to ρ_s , so it must be retained as a fitting parameter. This situation presents an additional difficulty in the regression analysis, in particular with the calculation of the residual, $\sum e^2$. Three options were considered:

Residual option 1

$$\sum e^2 = \sum_1^{n_1} (r(c^*) - \widehat{r(c)})^2 + \sum_1^{n_2} (r(c_\infty) - \widehat{r(c)})^2 \quad - 6$$

Residual option 2

$$\sum e^2 = \sum_1^{n_1} (r(c^*) - \widehat{r(c)})^2 + \sum_1^{n_2} \left\{ \frac{r(c_\infty)}{\rho_s} - \left\{ \frac{\widehat{r(c)}}{\rho_s} \right\} \right\}^2 \quad - 7$$

Residual option 3

$$\sum e^2 = \sum_1^{n_1} \left\{ \frac{r(c^*)}{\rho_s} - \left\{ \frac{\widehat{r(c)}}{\rho_s} \right\} \right\}^2 + \sum_1^{n_2} \left\{ \frac{r(c_\infty)}{\rho_s} - \left\{ \frac{\widehat{r(c)}}{\rho_s} \right\} \right\}^2 \quad - 8$$

Option 1 is the intuitive selection and is mathematically reasonably rigorous. However, its calculation requires the multiplication of the “measured” variable by one of the fitting parameters, ρ_s . This introduces significant un-intended consequences in the fitting process which is simply the

minimisation of $\sum e^2$ as a function of r_0 , ρ_s and n_{RZ} . In effect the set of the “measured” values pertaining to $r(c_\infty)$ is multiplied by a variable weight, ρ_s , whose magnitude depends on the success of the fitting process.

Option 2, whilst the simplest to implement has the effect of strongly biasing the fitting process towards the $r(c^*)$ data sub-set. As a consequence of the potential for systematic but variable bias option 2 was rejected.

Option 3 is broadly similar to option 1, however all the residuals are down weighted by the solids density. This option suffers from the same issues as option 1 and additionally it is susceptible to the floc density being set to zero during the course of the solution process. This final potential problem led to its rejection as a method.

Each of the options considered is based on a “scalar” characterisation of the residual. Such a characterisation implicitly assumes that the magnitude of the residual is independent of the measured value. Exploration of the impact of this assumption is warranted but is beyond the present scope.

Based on the option 1 residual the fitting process proceeded in a stagewise fashion. Commencing with n_{RZ} constrained to be zero and ρ_s constrained to an arbitrary value greater than the maximum concentration, 10^4 , for computational convenience. This calculation yields the summed residuals around the mean. A test fit with n_{RZ} constrained to 4.5 was then performed. The constrained value for n_{RZ} was arbitrarily chosen as the most commonly reported value in the engineering literature and has no physical significance beyond that in this context. The test fit was checked for its statistical significance using a standard “F” test at the 0.95 level. If accepted a further test fit with the constraint on the value of n_{RZ} was performed and the incremental statistical significance checked for significant improvement.

Step 3c

The filtration diffusivity is related to the coefficient on the exponent of the late phase model through the following expression

$$D(c_\infty) = M_L \frac{h_\infty^2}{\pi^2} \quad - 9$$

The functional form for the filtration diffusivity is defined by the combination of the first derivative of the particle stress model with the cake resistivity as follows:

$$D(c) = \frac{\rho_s P y'(c)}{r(c)} \quad - 10$$

The fitting processes outlined in sections 3a and 3b fully define the functional form and coefficients for the above expression. Therefore, only the residual around the proposed model is calculated in order to estimate the confidence band for the correlation of $D(c)$ versus c .

Parameter		Poly clay dose					
Poly clay dose		140 mg l ⁻¹		660 mg l ⁻¹		1600 mg l ⁻¹	
		Best fit value	Confidence limit (95%)	Best fit value	Confidence limit (95%)	Best fit value	Confidence limit (95%)
Hydraulic resistivity							
r_0	TPa s m ⁻²	110	2.6 747	2.5	0.4 14	2.4	0 1650
ρ_s	kg m ⁻³	3170	2393 4387	1520	1420 1675	1790	1540 4590
n_{RZ}	-	4.5	-	4.5	-	4.5	-
Particle stress							
n_v	-	4	2 5	7	6 8	6	2 10
B^*	kJ m ³ kg ⁻² K ⁻¹	-		-		-	
\mathcal{D}^*	kJ m ^{3(n_v-1)} kg ^{-n_v} K ⁻¹	9.93x10 ⁻¹⁴	9.09x10 ⁻¹⁴ 1.08x10 ⁻¹³	3.39x10 ⁻²²	3.30x10 ⁻²² 3.48x10 ⁻²²	1.67x10 ⁻¹⁹	1.45x10 ⁻¹⁹ 1.90x10 ⁻¹⁹

Table 3 Estimated parameter and material property values from

r_0 represents the hydraulic resistivity of a single isolated floc, equivalent to an infinitely dilute suspension. In sedimentation this can be related to the settling velocity of the isolated floc. r_0 is estimated with a poor degree of certainty. This arises principally from the relatively high and rather narrow range of concentrations which characterise the asymptotic filter cakes in conjunction with the very strong concentration dependence of the cake resistivity, $r(c_\infty)$

ρ_s represents a limiting concentration or “pole” at which the hydraulic resistivity of the cake goes to ∞ , i.e. the cake becomes completely impervious and no further filtration can take place. The magnitude of ρ_s is bounded at the lower limit by the density of the suspending fluid and at the upper limit by the density of the floc forming solids. ρ_s is estimated with somewhat greater certainty than r_0 being approximately +/- 20% at the 0.95 confidence level for the 140 mg l⁻¹ dose diminishing less than to +/- 10% at the 660 mg l⁻¹ dose.

Despite the low confidence in the individual estimates of r_0 the best fit values can be seen to diminish significantly as the polyclay dose is raised from 140 to 660 mg l⁻¹. This is indicative of a change in floc morphology towards the formation of “tighter” structures which are generally more-dense and less fractal. However as the “PolyClay” dose is increased through the same range it can also be seen that the magnitude of ρ_s diminishes significantly too. This implies that the internal structure of the floc has become less permeable. At low cake concentrations the internal permeability of the floc is not significant only becoming dominant during the late, “compression” phase, when the inter floc spaces have diminished. The transition from a dense “pole” to a less dense “pole” is indicative of the properties of the filter cake moving from domination by the paint properties to domination by the “PolyClay” properties. The limiting density at high “PolyClay” doses estimated here is consistent with the range of values found for bentonite “dumped” under natural ambient conditions of 1500 – 1800 kg m⁻³ [Sipag Bisalta 2020].

It is noted that both the paint solids and bentonite have distinct plate like structures. Thus it is expected that at low concentrations of “PolyClay” the paint solids will tend to orientate with increasing concentration to form cakes of relatively high hydraulic resistivity. However the addition of higher concentrations of poly clay will tend to disrupt the formation of orientated layers to some extent and where “PolyClay” is added in excess the residual, “un-reacted” bentonite would be

expected to orientate and form similar cakes for which the hydraulic resistivity rises sharply over a relatively narrow concentration range.

Equations of state, EoS, have their origins in describing the relationship between temperature, pressure and specific volume of an idealised substance, typified by the ideal gas. Here the concepts are adapted to describe the behaviour of the suspensions of solids. The virial EoS is applied as, at a mathematical level, it is a simple polynomial. Three terms have been used the first, linear, term describes “ideal” behaviour whilst the remaining pair describe deviation from the ideal. The coefficient of the linear term is then simply the product of the absolute temperature with a specific gas constant, \mathcal{R}^* . The second term, parabolic in concentration, provides the opportunity to create a minimum in the particle stress, P_y . The degree of final term, greater than 2, was determined by regression. The form of the EoS was further, arbitrarily, constrained to yield a minimum with a particle stress equal to zero. This minimum is termed the gel concentration. Once a value for \mathcal{R}^* has been established it is a simple matter to establish an indicative molecular weight for the solid flocs. The virial model proposed here can be considered to have an encapsulated power law model and the linear ideal model. The nature of the power law model however precludes the estimation of \mathcal{R}^* and thus an indicative molecular weight. The data collected in this work is such that the increment from the power law model to the 3 term virial model was not statistically significant and the latter was rejected making it impossible to determine values for the indicative molecular weight and gel concentration. Despite these limitations it can be seen that the exponent of the power law models increases significantly as the poly clay dose steps from 140 to 660 g m⁻³. This result reflects the changes in the hydraulic resistivity over the same range. The floc formed with the higher doses of “PolyClay” are generally “stronger” or better able to resist compression.

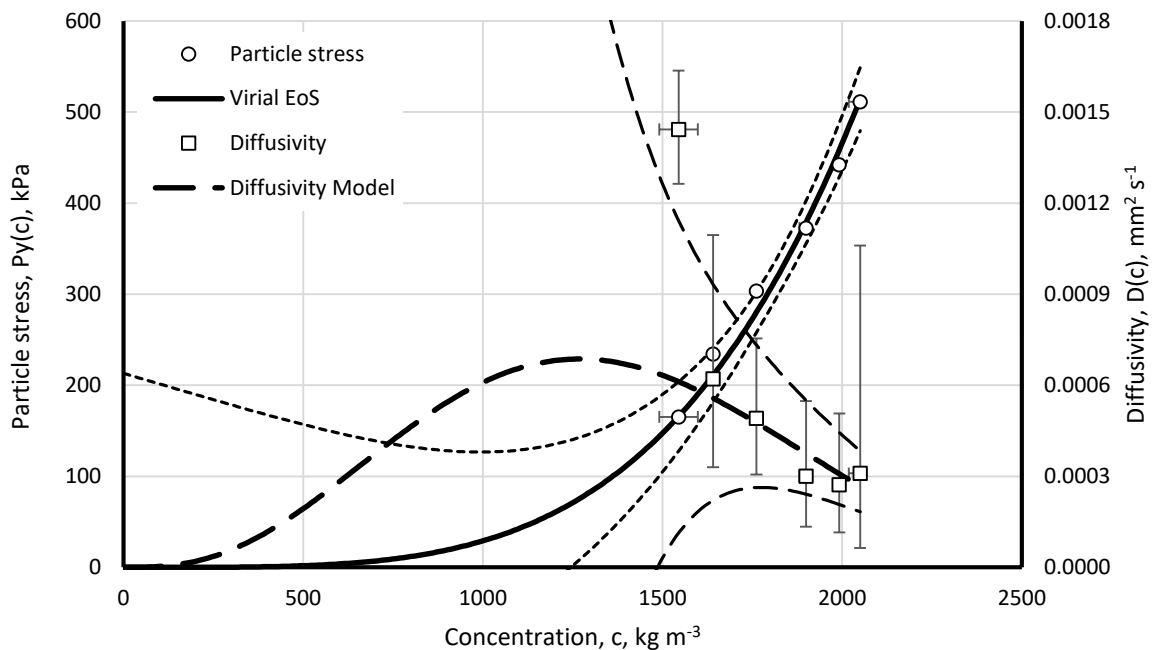


Figure 5 Particle stress and filtration diffusivity as functions of solids concentration for 4% paint residue adjusted to pH 6.3 with aluminium sulphate and dosed with 140 g m⁻³ “PolyClay”. Heavy lines indicate the results of systematic regression analysis and the light dashed lines indicate the 0.95 confidence bands of correlation to the models. Horizontal and vertical error bars indicate the 0.95 confidence intervals in the data estimates

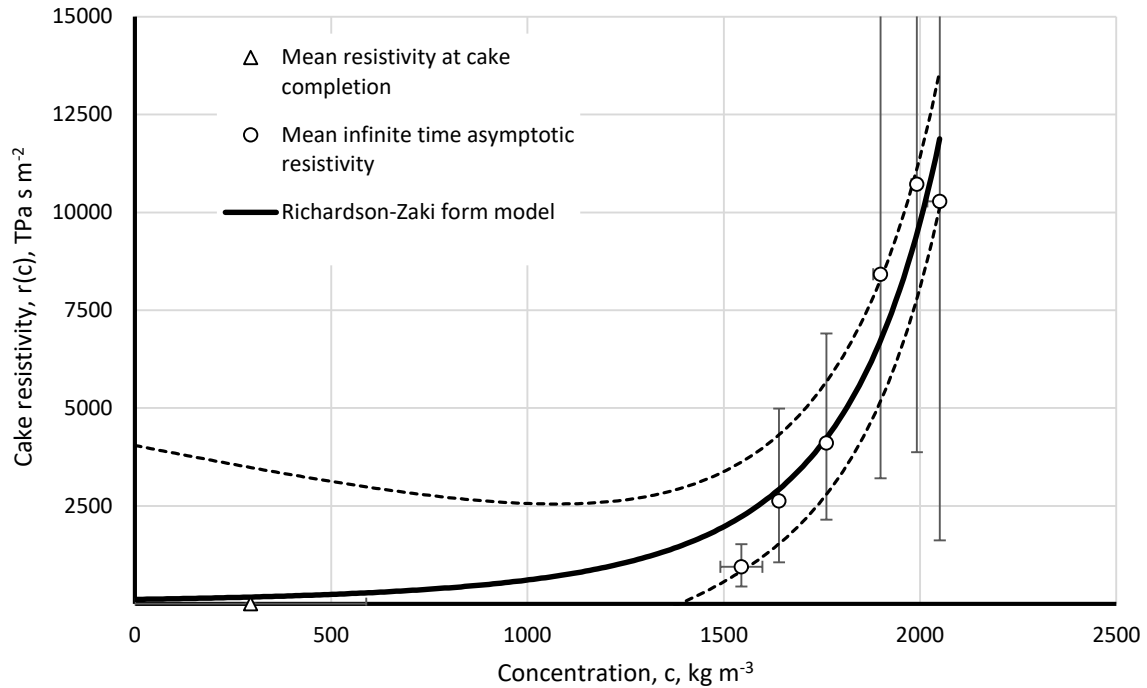


Figure 6 Filter cake resistivity as a function of solids concentration for 4% paint residue adjusted to pH6.3 with aluminium sulphate and dosed with 140 g m⁻³ “PolyClay”. Heavy continuous line indicates the results of systematic regression analysis and the light dashed lines indicate the 0.95 confidence band of correlation to the model. Horizontal and vertical error bars indicate the 0.95 confidence intervals in the data estimates.

From Figure 5, showing the particle stress and the filtration diffusivity as functions of concentration, it can be seen that the measured stress is determined to a high degree of confidence due entirely to the method by which the load is applied to the press. However there is hidden uncertainty in this determination potentially arising from “stiction” in the piston mechanism, as the load transmitted to the suspension was not measured directly. The horizontal error bars indicating uncertainty in the determination of the asymptotic solids concentration arise from the propagation of uncertainty in the determination of the asymptotic piston height in step 2 of the regression process. The certainty in the determination of this parameter improves as the inter step travel of the piston diminishes. The indicated confidence is much lower for the filtration diffusivity than the particle stress. This arises from its dependence on both the estimate of the asymptotic piston height and on the exponential, “rate” term, M_L . Confidence in the estimation of M_L diminishes with decreasing inter step piston travel. Thus for the final pressure increment, where the piston travel was approximately 40 μm , the 0.95 confidence interval is particularly large. The estimated filtration diffusivity can be seen to pass through a maximum of approximately 0.007 mm² s⁻¹ at a solids concentration of approximately 1250 kg m⁻³, below the range of the collected data. Maximising the filtration diffusivity can be used as an objective of the addition of flocculants. In this work the qualitative effect of the addition of “PolyClay” is to increase the maximum value of $D(c)$ but this is achieved at the cost of decreasing the concentration at which the maximum occurs and in the range for which data was collected the effect of “PolyClay” addition is to reduce the filtration diffusivity thus making the dewatering process less effective. Over the concentration range of interest (>1250 kg m⁻³) $D(c)$ can be seen to decrease with increasing concentration. This is an indication that a technology which

is counter current in character, i.e. water and solids move in opposite directions, may be more suitable for this dewatering process. In this case, should the required forces be achievable, centrifugation represents a candidate, counter current technology.

Figure 6 shows the hydraulic resistivity of the cake as a function of concentration. The large confidence intervals characterising the data shows a very high degree of uncertainty. This arises from the dependence of the data values on ρ_s and the first derivative of the EoS, $Py'(c)$, in addition to both M_L and h_∞ . Table 3 shows that ρ_s is characterised by relatively wide 0.95 confidence limits, particularly the upper confidence limit.

Conclusions

This work has shown that the addition of “PolyClay” as a filter aide for paint waste reduces the hydraulic resistivity at lower concentrations and increases it at higher concentrations whilst simultaneously increasing the particle stress. Together these have a combined deleterious effect on the time and energy required to dewater the waste to high solids concentration by filtration. The results also show that a significant change in suspension behaviour occurs between the “PolyClay” doses of 140 mg l^{-1} and 660 mg l^{-1} and that further changes up to “PolyClay” doses of 1600 mg l^{-1} are more modest. It may be concluded that there is an opportunity to reduce “PolyClay” dose into a range between 10% and 50% of current manufacturing practice. In addition this work indicates that alternative, centrifuge based, technology is worthy of investigation. The data interpretation method enables different flocculant materials to be more rapidly screened and more appropriately screened than conventional jar tests and large scale filtration trials.

Acknowledgements

The authors gratefully acknowledge the support of the Innovate UK, Knowledge Transfer Partnership (KTP) Grant No. KTP10134.

Nomenclature

		Dimensions
$B_{L,n}$	Coefficient of the nth term of Landman et al’s late phase series solution	-
B^*	Specific coefficient of 2 nd term of virial solids stress model	$\text{L}^5 \text{M}^{-1} \theta^{-1}$
C	Coefficient of time independent terms fitting algorithm	variable
c	Solids concentration	M L^{-3}
c^*	Diffusivity weighted mean concentration at cake completion	M L^{-3}
\tilde{c}_{gel}	Gel concentration derived from virial solids stress model	M L^{-3}
D	Filtration diffusivity	$\text{L}^2 \text{T}^{-1}$
\mathcal{D}^*	Specific coefficient of the nth term of virial solids stress model	variable
DoF	Degrees of freedom	-
E^2	Sum of squared residuals	variable
F	Fisher distribution	-
h	Measured height of filter piston above filter membrane	L
\hat{h}	Model estimated height of filter piston above filter membrane	L
M	Fitted coefficient of time dependent terms in fitting algorithm	variable
M^*	Nominal molecular mass of solid structures	M
n_{RZ}	Richardson and Zaki model exponent	-
n_v	Exponent of the n th term of virial solids stress model	-
ΔP	Filtration applied differential pressure	$\text{M L}^{-1} \text{T}^{-2}$
Py	Concentration dependent inter particle stress	$\text{M L}^{-1} \text{T}^{-2}$

Py'	Concentration dependent inter particle stress gradient	$L^2 T^{-2}$
\mathcal{R}^*	Nominal specific gas constant	$\text{kJkg}^{-1} \text{K}^{-1}$
r	Concentration dependent hydraulic resistivity	$\text{M L}^{-3} \text{T}^{-1}$
r_0	Hydraulic resistivity of infinitely dilute suspension	$\text{M L}^{-3} \text{T}^{-1}$
T	Absolute temperature	θ
t	Elapsed time	T

Greek symbols

α	Cake completion parameter	-
ρ_s	Solids density	M L^{-3}

Subscripts

0	Initial (time zero)
∞	Infinite time asymptote
C	Pertaining to the moment of cake completion
$crit$	Critical value relating to rejection criteria in “F” and “t” tests
E	Early (cake growth) phase
L	Late (cake compression) phase
N	Number of fitted parameters
R	Pertaining to a stepped pressure run
RZ	Richardson and Zaki
s	Solid phase
$stat$	Statistic relating to “F” and “t” tests
U	Unweighted
v	virial

References

Auzerais, F. M., R Jackson, and W. B. Russel, 1988

The Resolution of Shocks and the Effects of Compressible Sediments in Transient Settling, *J. Fluid Mech.*, 196, 437 (1988).

Buscall, R. & White, L. R. 1987

The consolidation of concentrated suspensions. Part 1.—The theory of sedimentation. *J. Chem. Soc. {,} Faraday Trans. 1* **83**, 873–891 (1987).

CTECH Europe Ltd, Rovert House, Water Tower Road, Clayhill Business Park, Neston CH64 3US, dis-United Kingdom

“PolyClay” is a bentonite based product:

<http://ctech.design365hosting2.co.uk/products/polyclay-wastewater-treatment-products/>

Accessed: Oct 2020

De Kretser, R., S. P. Usher, P. J., Scales, K. A., Landman, and D. V. Boger, 2001

Rapid Filtration Measurement of Dewatering Design and Optimisation Parameters,” *AIChE. Journal*, 47(8), 1758 (2001).

Green, M. D., Landman, K. A., De Kretser, R. G. & Boger, D. V. 1998

Pressure filtration technique for complete characterization of consolidating suspensions. *Ind. Eng. Chem. Res.* 37, 4152–4156 (1998).

Kemmer, G., and S. Keller, 2010

Nonlinear least-squares data fitting in Excel spreadsheets,

Nature Protocols 5, 267 - 281 (2010), Published online: 28 January 2010,
doi:10.1038/nprot.2009.182

Kynch G. J., 1952

A Theory of Sedimentation

Transactions of the Faraday Society, Volume 48, 1952, pp 166 -176

Landman, K. A. & White, L. R. 1994

Solid/liquid separation of flocculated suspension,.

Adv. Colloid Interface Sci. **51**, 175–246 (1994).

Landman, K. A., and L. R. White, 1997

Predicting Filtration Time and Maximizing Throughput in a Pressure Filter,

AIChE. Journal, 43(12), 3147 (1997)

Richardson, J. F., and W. N. Zaki, 1954

Sedimentation and Fluidisation: Part1,

Trans. Inst. Chem. Engs., 32, 35 (1954).

Sipag Bisalta, <http://www.sipagbisalta.it/en/>

[http://www.bentonite.it/what-is-](http://www.bentonite.it/what-is-bentonite.php#:~:text=Its%20density%20when%20dry%20varies,to%201.8%20g%2Fcm%203)

[bentonite.php#:~:text=Its%20density%20when%20dry%20varies,to%201.8%20g%2Fcm%203](http://www.bentonite.it/what-is-bentonite.php#:~:text=Its%20density%20when%20dry%20varies,to%201.8%20g%2Fcm%203).

Accessed: Oct 2020

Usher, S. P., De Kretser, R. G. & Scales, P. J. 2001

Validation of a new filtration technique for dewaterability characterization.

AIChE J. **47**, 1561–1570 (2001).